Revista GEOCIÊNCIAS

unesp

ISSN: 1980-900X (online)

GEOCHEMISTRY AND MINERALOGY OF THE BANDED IRON FORMATION, WEST MOEDA SYNCLINE, QUADRILÁTERO FERRIFERO REGION

GEOQUÍMICA E MINERALOGIA DA FORMAÇÃO FERRÍFERA BANDADA DA PORÇÃO OCIDENTAL DO SINCLINAL MOEDA, REGIÃO DO QUADRILÁTERO FERRÍFERO

Jorge RONCATO, Letícia dos Santos BARBOSA, Guilherme Henrique RIBEIRO, Kaio Felipe MENDES, Marcos Vinicius Monteiro CARVALHO, Rodrigo Sérgio de PAULA, Luiz Guilherme KNAUER

Universidade Federal de Minas Gerais. Instituto de Geociências. Avenida Antônio Carlos, 6.627 – Pampulha. Belo Horizonte – MG.
E-mail: roncato@ufmg.br; le_sbarbosa@hotmail.com; ghribeiro50@gmail.com; kaiofelipe.mendes@gmail.com; marcos.monteiro@vallourec.com; rodrigo.spdm@yahoo.com.br; gknauer@gmail.com

RESUMO - No flanco oeste do Sinclinal Moeda, a Formação Ferrífera Bandada apresenta litotipos com variados graus de enriquecimento: Hematita (>=64 wt.% Fe), Itabirito Rico (58 a 64 wt.% Fe), Itabirito Intermediário (45 a 58% em peso Fe), Itabirito Pobre (20 a 45% em peso Fe), Itabirito Limonítico Pobre (20 a 45 wt.% Fe), Itabirito Limonítico Intermediário (45 a 58 wt.%Fe) e Itabirito Rico em Manganês (20 a 45 wt.% Fe). A sequência metassedimentar é estratigraficamente correlacionável com filitos e quartzitos do Grupo Caraça da base do Supergrupo Minas. A estratificação sedimentar/diagenética da Formação Ferrífera Bandada metamorfizada (itabiritos da Formação Cauê) é geralmente transposta por uma xistosidade planar. Os 76 furos de sondagem realizados entre 2005 e 2014, e nove amostras adicionais retiradas do depósito foram classificadas em diferentes fácies de itabiritos com base no grau de enriquecimento em ferro, alumínio e manganês nas análises químicas, e o grau de compactação do material, resultando em 11 litotipos diferentes (com seus respectivos valores médios de ferro). Litotipos com um teor de Al_2O_3 acima de 2% são chamados Limoníticos, e aqueles acima de 1% de Mn são Manganês. Estudos de XRD e microscopia óptica indicam uma composição mineralógica de quartzo, hematita granular, goethita e uma mistura muito fina de óxidos e hidróxidos de ferro (material limonítico). Os diversos e extensos litotipos apresentam dificuldades consideráveis para exploração, bem como oportunidades em relação a diferentes meios de amostragem e à formação de recursos. O desenvolvimento de compreensão geoquímica apropriada é extremamente importante para um melhor planejamento exploratório. Estes dados visam fornecer uma introdução concisa à geologia do minério da parte de depósitos de minério de ferro no Sinclinal Moeda.
Palavras-chave: Minério de ferro. Região do Quadrilátero Ferrífero. Metalogênese. Geoquímica. Mineralogia. DRX.

ABSTRACT - At the western flank of Moeda Syncline, a BIF-hosted with variable grades lithotypes: Hematite (>=64 wt.% Fe), Rich Itabirite (58 to 64 wt.% Fe), Intermediáte Itabirite (45 to 58 wt.% Fe), Poor Itabirite (20 to 45 wt.% Fe), Poor Limonitic Itabirite (20 to 45 wt.% Fe), Intermediate limonitic Itabirite (45 to 58 wt.% Fe) and Manganese-rich Itabirite (20 to 45 wt.% Fe). The metasedimentary sequence is correlatable with phyllites and quartzites of the Caraça Group at the base of the Minas Supergroup. The sedimentary/diagenetic bedding of the metamorphosed BIF (itabirites of the Cauê Formation) is generally transposed by a planar schistosity. The 76 drill holes carried out between 2005 and 2014, and nine additional samples taken from the deposit were classified into different facies of itabirite based on the degree of enrichment in iron, aluminum, and manganese in the chemical analyses, and the degree of compactness of the material, resulting in eleven different lithotypes (with their respective average iron values). Lithotypes with an Al_2O_3 content above 2% are called Limonitic, and those above 1% of Mn are Manganese. Both XRD and optical microscopy studies indicate a mineralogical composition of quartz, granular hematite, goethite, and a very fine-grained mixture of iron oxides and hydroxides (limonitic material). The diverse and extensive lithotypes pose considerable difficulties for exploration - as well as opportunities regarding different sample media and the formation of resources within them. The development of appropriate geochemical understanding is exceedingly important for better exploratory planning. This data aims to provide a concise introduction to the ore geology of the part of Moeda Syncline iron ore deposit.
Keywords: Iron ore. Quadrilátero Ferrífero Region. Metalogenesis. Geochemistry. Mineralogy. XRD.

INTRODUCTION

The Moeda Syncline (Figure 1) is a significant source of iron ore in the Cauê Formation, which composed of banded iron formations (Sousa, 2016). The local banded iron formation comprises medium to coarse-grained granoblastic magnetite orebodies situated in contact with Proterozoic units of the Minas Supergroup (Figure 2). The Itabirite samples are characterized by intercalation between levels consisting of iron oxides, with some content in magnetite, and levels consisting of quartz, with a thickness of millimeters. It has variable characteristics and may present massive or banded structures.

The Moeda Syncline (Figure 2) is characterized by constituting a geometric and kinematic arrangement of an epidermal tectonic (thin-skin), involving the Greenstone units of the Rio das Velhas Supergroup and the Minas Supergroup on the basal surface, followed by a tectonic fore country basement (thick-skin) with the involvement of the metamorphic complexes Bonfim and Bação (Castro et al., 2020). In this paper, we aim to conduct a detailed study on the classification of itabirites, taking into account iron content, manganese anomalies, and the presence of rocks with pelitic bands containing high Al_2O_3.

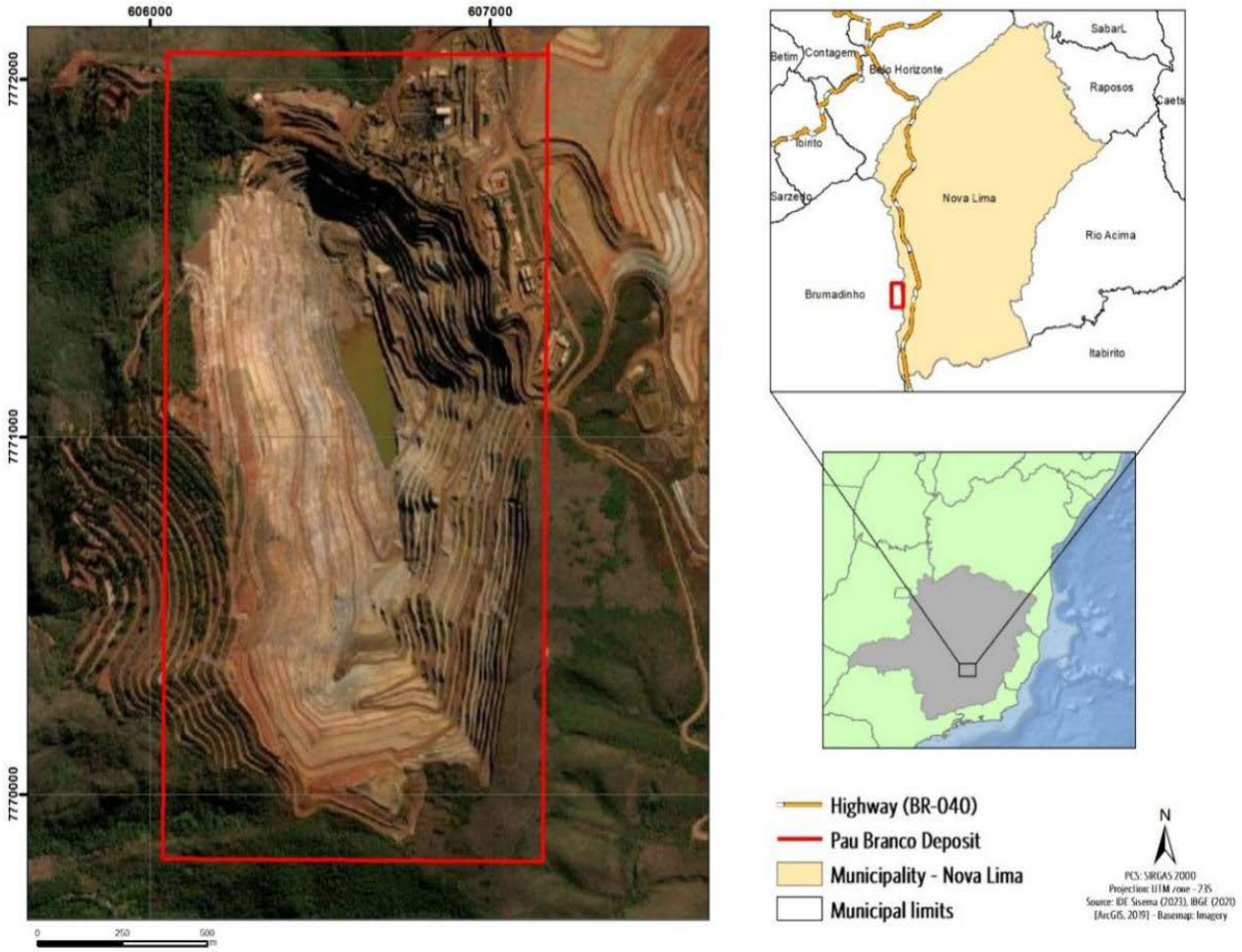

Figure 1 - Location of the Moeda Syncline and aerial view of the pit of Pau Branco Deposit.

Geological context

The investigated area is located in the Northern Portion of Moeda Ridge, approximately 17 km south of the state capital, Belo Horizonte, Minas Gerais, Brazil (Figure 1). The Quadrilátero Ferrífero region (QF; Figures 1 and 2) is situated in the southern portion of the São Francisco craton (Almeida, 1976) and is composed of the Archean Rio das Velhas greenstone belt (Schorscher et al., 1982), the Paleoproterozoic Minas Supergroup and the Itacolomi Group.

Granite-gneiss domes (Dorr, 1969, Herz, 1970, Lana et al., 2013), which Consist of poly-deformed rocks, surround these supracrustal units.

The Rio das Velhas Supergroup consists of a sequence of metavolcanosedimentary rocks. Associated by Almeida et al. (1976) and Schorscher (1976) to Archean Greenstones belts

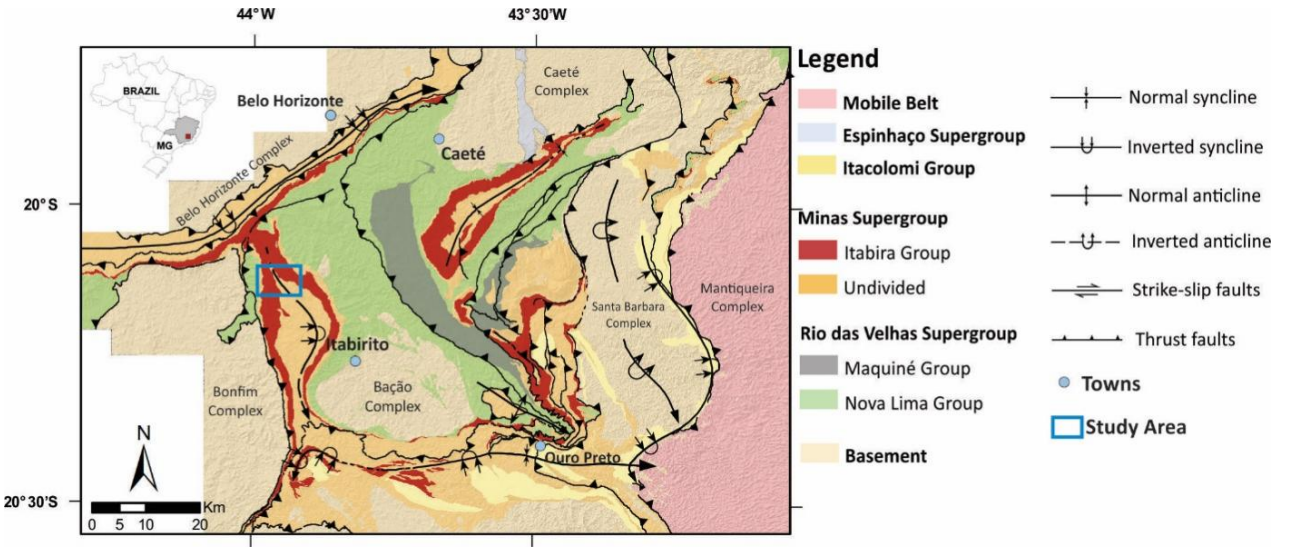

Figure 2 - Simplified geological map of the Quadrilátero Ferrífero. Modified from Costa et al. (2022).

characterized by mafic, ultramafic, volcanic and vulcanoclastic rocks, involving immature classical sediments (Dorr et al., 1957; Dorr, 1969; Roncato et al., 2015, 2020, 2023). The Minas Supergroup consists of Archean and Paleoproterozoic metasedimentary rocks of chemical and clastic origin (Babinski et al. 1991, 1995, Renger et al., 1994, Hartmann et al., 2006, Cabral et al., 2012, Koglin et al., 2014). According to Alkmim & Martins-Neto (2012), this lithostratigraphic unit comprises two sequences separated by a regional discordance.

In the Itabira Group, the Cauê Formation (Dorr, 1969; Klein & Ladeira, 2000) consists essentially of itabirites and has great importance in QF due to the world-class iron ore deposits (Rosière et al., 2008). The Gandarela Formation is composed of dolomites and limestones, enriched in iron and with preserved stromatolites (Souza & Müller, 1984).

The structural evolution of the QF region took place in three main periods during the Rio das Velhas Orogeny (Zucchetti & Balthazar, 2000 e Balthazar & Zucchetti, 2007): between 2.8 and 2.67 Ga, which relates to the evolution of the Rio das Velhas greenstone belt; 2.10 to 1.90 Ga, the Transamazonian event; and the Brasiliano orogeny (Sepulveda et al., 2021).

The stratigraphic units of the *Moeda Syncline* (here mainly represented by Pau Branco Deposit geology) consist of the Batatal and Cauê formations, both belonging to the Minas Supergroup (Figure 2). The Batatal Formation reaches thicknesses exceeding 80 m and is mainly composed of sericite-rich phyllite. On the other hand, the Cauê Formation is the main stratigraphic unit, with a minimum thickness of 250 m and being in transitional contact with the Batatal Formation. The predominant lithotype was classified as siliceous itabirite, which occurs intercalated with manganese itabirites, limonitic itabirites, and hematitic bodies. Specular hematite occurs associated with shear zones and quartz veins (Hensler et al., 2014; Mendes, 2015). These units are occasionally cut by mafic dikes, which have metric thicknesses and are characterized by an advanced stage of weathering and obliteration of primary structures (Grossi-Sad, 2005). Covering the described units are recent colluviums and colluvial deposits, observed in the topographically higher portions.

Regarding the morpho-structural context, the study área is on the western flank of Moeda Syncline, a megastructure that extends for 40 km on the western boundary of the QF, from its junction with the Serra do Curral to its fusion to the south with the Dom Bosco Syncline (Figure 2). It has an N-S axial direction, with the western flank dipping regularly to the east at angles between 30º-45º and the eastern flank being subvertical or inverted with a high dip (Dorr, 1969). The Pau Branco Deposit (PB) is present in a north-south elongated ore body, where the west slopes are predominantly sustained by phyllites of the Batatal Formation dipping towards the center of the pit. Two types of iron ores are described, namely, hematite-rich ore bodies located in the central part of the open pit, and schistose itabirite in the eastern part of the pit.

The quartz itabirite is the main lithotype, intercalated locally with dolomitic itabirite. Both types of itabirites are enriched in iron, ranging

from 45 to 70 % Fe. The high grade ore forms bedding-concordant bodies (Hensler et al., 2014; Mendes et al., 2017). The iron ore occurs as friable, supergene orebodies with 58–64 % Fe and as hard ore lenses with 64–70 % Fe. Specularite occurs in shear zones and forms monomineralic hydrothermal veins that crosscut the iron orebodies but also occurs in association with quartz veins (Mendes et al., 2017). Dominant iron oxide is martite, with relicts of kenomagnetite (Hensler et al., 2014). Along a reverse shear zone at the contact with the underlying Caraça Group, a metre-thick, phyllitic zone was mineralised, consisting mainly of microplaty hematite. Within this zone, idiomorphic, up to 1 cm diameter, magnetite crystals were formed (Hensler et al., 2014).

According to recent internal information, the iron content varies from 20% to 64%. The Pau Branco Deposit team organizes the ore types according to iron content as described below; if it contains 20-45% of Fe, the iron ore is considered poor, if it contains between 45-58% of Fe, the iron ore is considered intermediate, and if it contains between 58-64% of Fe, the iron ore is considered rich. It may also vary in terms of compactness, being categorized as soft, semi-compact, or compact, successively.

Besides the other ore lithologies that feed the beneficiation plant, such as hematite rock (Figure 3; with an Fe percentage above 64%), the limonitic itabirite is mentioned, which has a poor to intermediate Fe content and over 2% of aluminum oxide; and the manganese itabirite, which tends to be poor in Fe and has over 1% of manganese oxide.

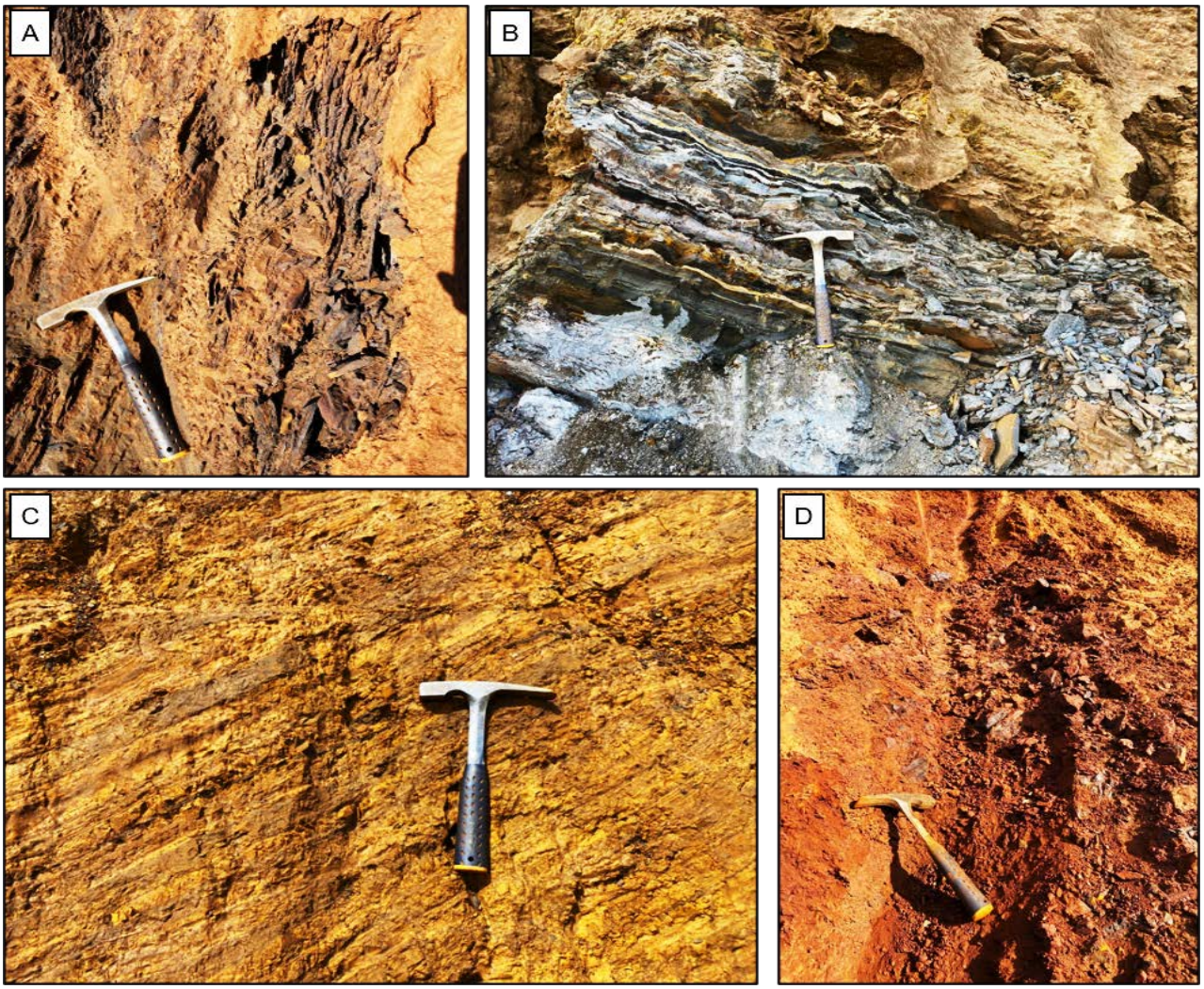

Figure 3 - Main types of ore in the region. A) Hematite rock. B) Siliceous itabirite. C) Limonite itabirite. D) Fe-rich colluvium.

The iron mineralization of the deposit is both supergene and hypogene (Hensler et al., 2014). The ore minerals include hematite (sometimes specular), martite, and magnetite, along with hydrated iron oxide minerals like goethite and limonite. Other minerals commonly present in these rocks are quartz, gibbsite, and kaolinite, when aluminum is present in the system and

influenced by hydration processes, as well as dolomite and amphiboles, which are rare to preserve on the surface due to weathering in the region (Grossi-Sad, 2005).

MATERIAL AND METHODS

Sampling and Analytical Procedures

We collected itabirite and iron ore samples from eleven different points located in the Pau Branco Deposit. The iron ore samples were analyzed for petrographic thin section, geochemical analysis, X-ray diffraction analysis and Binocular loupe analysis as summarized in the table 1.

The samples sent for X-ray diffraction (DRX) resulted in diffractograms obtained using a Panalytical Expert PRO diffractometer adapted for powdered polycrystalline samples. The software used for data processing was HighScore Plus. The COD - Crystallography Open Database, provide the phase identification database. For geochemical studies, the listed samples were analyzed in the internal laboratory of Vallourec Mineração. The analytics were conducted in the XRF Laboratory of CPMTC-UFMG.

Table 1 - Summary of the sampling and analysis.

POINT	CODE	FIELD LITHOTYPE	PROCEDURES
TG001	AE22072 (TG001)	Manganese Itabirite	Chemical analysis
	AE22076 (TG001)		Duplicate chemical analysis
	TG001		X-ray diffraction analysis
	TG001		Petrographic thin section
TG002	AE22073 (TG002)	Rich Manganese Itabirite	Chemical analysis
	AE22077 (TG002)		Duplicate chemical analysis
	TG002		X-ray diffraction analysis
	TG002		Petrographic thin section
TG003	TG003-01	Soft Poor Limonite Itabirite	X-ray diffraction analysis only in the limonitic band
	TG003-01		Binocular loupe analysis only in the limonitic band
	AE22078 (TG003-02)		Chemical analysis only in the limonitic band
	TG003-03		Petrographic thin section only in the limonitic band
TG004	TG004		X-ray diffraction analysis
	TG004-01		Binocular loupe analysis only in the limonitic band
	TG004-02		Binocular loupe analysis, only in the ferrous band
	AE22079 (TG004-03)		Chemical analysis
TG005	TG005-01	Semi-compact Intermediate Itabirite	Petrographic thin section
	TG005-02		Binocular loupe analysis
TG006	TG006-01	Soft Intermediate Limonite Itabirite	Binocular loupe analysis, only in the ferrous band
	TG006-02		Binocular loupe analysis, only in the silicosa band
	TG006-03		Binocular loupe analysis only in the limonitic band
	AE22080 (TG006-04)		Chemical analysis
	TG006-05		Petrographic thin section
	TG006-06		X-ray diffraction analysis in the silicosa band
	TG006-07		X-ray diffraction analysis in the limonitic and ferrous band
TG007	TG007-01	Intermediate Soft Itabirite	Petrographic thin section
	TG007-02		Binocular loupe analysis, only in the ferrous band
	TG007-03		Binocular loupe analysis only in the limonitic band
TG008	AE22081 (TG008)	Semi-compact Intermediate Itabirite	Chemical analysis
	TG008-01		Petrographic thin section
	TG008-04		Petrographic thin section
TG009	TG009	Compact Intermediate Limonite Itabirite	Petrographic thin section
TG010	TG010		Petrographic thin section
TG011	AE22084 (TG011)		Chemical analysis
	TG011		Petrographic thin section

Table 2 summarizes the current lithologies, associating them with ore lithotypes according to iron, aluminum and manganese content and the local symbols used to name each lithotype.

Table 2 - Iron ore lithotypes and associated Fe, Al and Mn contents (Soft=B, Semi-compact=S and Compact=C).

IRON ORE LITHOTYPE	SYMBOL	FIELD LITHOTYPE	%Fe	%Al_2O_3	%MnO
Soft Hematite	HEB	Hematite (HE)	>=64	-	-
Semi-compact Hematite	HES				
Compact Hematite	HEC				
Soft Rich Itabirite	IRB	Rich Itabirite (IR)	58%,64%	-	-
Semi-compact Rich Itabirite	IRS				
Compact Rich Itabirite	IRC				
Soft Intermediate Itabirite	IIB	Intermediáte Itabirite (II)	45%,58%	<=2	-
Semi-compact Intermediate Itabirite	IIS				
Compact Intermediate Itabirite	IIC				
Soft Poor Itabirite	IPB	Poor Itabirite (IP)	20%,45%	>2	-
Semi-compact Poor Itabirite	IPS				
Compact Poor Itabirite	IPC				
Soft Poor Limonite Itabirite	ILPB	Poor Limonitic Itabirite (ILP)	20%,45%		
Semi-compact Poor Limonite Itabirite	ILPS				
Compact Poor Limonite Itabirite	ILPC				
Soft Intermediate Limonite Itabirite	ILIB	Intermediáte limonitic Itabirite (ILI)	45%,58%	>2	-
Semi-compact Intermediate Limonite Itabirite	ILIS				
Compact Intermediate Limonite Itabirite	ILIC				
Soft Rich Manganese Itabirite	IMB	Manganese rich Itabirite (IM)	20%,45%	-	>=1
Semi-compact Rich Manganese Itabirite	IMS				
Compact Rich Manganese Itabirite	IMC				
Hard lateritic cap ("canga")	CGM	Iron ore covering	-	-	-
Colluvium/eluvium	CEL				
Sedimentary breccia	BRS				

Petrographic Studies

Six strategic iron ore lithotypes were sampled and described according to the petrologic characteristics and mineralogy (Tables 1 and 2; HES, IRB, IIB, IIS ILPB, ILIB and IMB).

The HES is characterized by its close association with the phyllites of the Batatal Formation. It appears as a brecciated-looking itabirite, featuring intercalated iron-enriched bands and limonitic bands ranging from millimeter to centimeter scale. The rock exhibits a dark color, indicating significant iron enrichment, with sandy limonitic bands occurring more sporadically compared to limonitic itabirites. It has a very fine grain size, granoblastic texture, and generally lacks well-defined banding.

The IRB is characterized as a friable itabirite with a dark to ocher color, primarily comprising centimeter-scale bands of black to black-purple color interspersed with millimeter to centimeter-scale yellow ocher-colored clayey bands. It is predominantly composed of a limonitic matrix (85%), described as a clayey mass with an orange color, containing fine to anhedral goethite crystals.

The IIB is characterized by a fine grain size and granoblastic texture, with banding marked by a limonitic matrix. Hematite (35%) occurs as fine, subhedral to euhedral crystals with a light gray color, while goethite (15%) is present in the form of subhedral crystals with a bluish-gray color, often associated with hematite.

The IIS is described based on drilling cores (TG009, TG010, and TG011) and point TG005. The lithotypes are described as semi-compact rocks with well-defined banding composed of centimeter-scale ocher-colored argillaceous-silt bands, dark Fe-enriched bands with metallic luster, and, to a lesser extent, millimeter-scale quartzitic bands. The rock is characterized as fine-grained granoblastic rocks with well-defined banding.

The ILPB occurs in gradational contact with siliceous and rich itabirites. It is characterized by the centimeter-scale sandy layers composed of quartz and hematite, alternating with decimeter-scale pelitic layers of ocher color and limonitic composition. Millimeter-scale quartz layers may occur in small quantities.

The predominant feature is the limonitic layers, which consist of fine-grained, inequigranular granoblastic rock. These layers are primarily composed of anhedral quartz grains enveloped in a microcrystalline limonitic and goethite matrix, with colors ranging from brown to orange. Locally, an incipient banding can be observed, marked by levels of quartz and limonitic microcrystals.

The ILIB is characterized by the intercalation of iron-rich bands ranging from centimeters to decimeters, limonitic pelitic bands of yellow ocher color, and white siliceous bands, with dimensions ranging from millimeters to centimeters.

In contrast to ILPB, ILIB presents a greater predominance of ferruginous bands. It is described as fine-grained, granoblastic, and without evident banding.

The compact intermediate limonite itabirite is described only at depth, through drill holes. Three core intervals were described and named as samples TG009, TG010, and TG011.

The lithotypes are described as compact rocks, with evident banding comprising intercalations of millimeter to centimeter bands of fine ocher-colored silty clay material, dark bands with metallic luster and enrichment in Fe, and, less frequently, millimeter-sized quartz bands with a white color.

Rock geochemistry

Rock samples from open pit and drill core, were selected for major oxide element (Fe, Mn, SiO_2, Al_2O_3, P, CaO, MnO, TiO_2, and PPC; Tables 3 and 4) geochemistry. Geochemical historical data are presented in table 4. Additionally, nine recent analysis samples taken for this work were added to this discussion, and are presented in table 3.

Eight samples collected at strategic points in the pit, and one sample from a drilling hole (TG011), were chemically analyzed to characterize the itabirites studied. The results with the percentage chemical composition of the rocks sampled are presented in table 3.

Table 3 - Values of itabirite analyses, at strategic points in the deposit pit.

ID	Point	Lithology	% Fe	% Mn	% SiO_2	% Al_2O_3	% P	% Cao	% MgO	% TiO_2	% PPC
AE22072	TG001	IMB	60.64	0.304	4.8	1.04	0.159	0.022	0.082	0.086	6.12
AE22076			61.18	0.249	3.52	1.32	0.168	0.022	0.106	0.093	5.92
AE22073	TG002	IMB	61.31	0.302	4.46	1.28	0.135	0.021	0.088	0.111	6.42
AE22077			60.65	0.291	3.41	1.68	0.213	0.021	0.123	0.125	6.44
AE22078	TG003	ILPB	24.13	0.191	53.66	4.83	0.161	0.019	0.226	0.104	6.96
AE22079	TG004	ILIB	58.87	0.119	4.16	0.91	0.147	0.016	0.064	0.035	8.94
AE22080	TG006	ILIB	46.07	0.14	29.78	2.55	0.078	0.013	0.21	0.045	2.35
AE22081	TG008	IIS	64.00	0.125	3.4	2.03	0.085	0.014	0.099	0.097	2.62
AE22084	TG011	ILIC	46.25	0.23	29.52	0.15	0.039	0.013	0.006	0.013	4.6
Average			53.68	0.22	15.19	1.75	0.13	0.02	0.11	0.08	5.60

The nine BIF samples analyzed in this study exhibit a higher average concentration of Fe (c. 53 wt%) compared to the average Fe concentrations reported for Algoma or Superior type deposits (c. 28 wt%, e.g. Gross and McLeod, 1980). These BIFs demonstrate highly variable SiO2 values ranging from 3 to 53% by weight (Table 3), with the Soft Poor Limonite Itabirite (ILPB) sample representing the highest value (ILPB) sample.

Most BIF samples are characterized by an average Al_2O_3 content (0.91 to 4.83 wt%) in comparison with data of Superior or Algoma type deposits (1.5–3.7 wt%; e.g. Gross and McLeod, 1980), the highest values here, with the Soft Poor Limonite Itabirite (ILPB) sample also showcasing.

For most silicate/ oxide facies BIF samples, CaO ranges from 0.01 to 0.02 wt%, MgO ranges from 0.01 to 0.23 wt%, the highest values here, also, represented by the Soft Poor Limonite Itabirite (ILPB) sample. TiO_2 ranges from 0.01 to 0.13 wt%. PPc ranges from 2.35 to 28.94 wt% (average 5.60).

The geochemistry of the following rocks was analyzed separately based on, according to the Fe enrichment content (Table 4).

Typical itabirites, banded rocks that intersperse light bands commonly siliceous and dark bands rich in Fe minerals, are subdivided according to their iron enrichment. Poor itabirites are defined as those that have between 20 and 45% Fe in their composition and can be friable, semi-compact, or compact.

The IPB and IPC are the exclusive where the average silica concentrations are higher than that of iron (Fe). Among the other lithotypes, aluminum (Al) has the lowest concentration value, and a trend also observed for Magnesium (Mg), Calcium (Ca) titanium (Ti), and phosphorus (P). The two lithotypes displays a very similar elemental distribution.

Table 4 - Average percentage values of itabirite analyses, according to the database.

Lithology	% Fe	% Mn	% SiO_2	% Al_2O_3	% P	% CaO	% MgO	% $Ti0_2$	PPC
HEB	66.06	0.19	2.5	1.07	0.08	0.04	0.07	0.06	1.8
HES	66.24	0.11	2.48	1.04	0.09	0.04	0.06	0.06	1.87
HEC	66.71	0.16	1.7	0.68	0.08	0.03	0.06	0.06	1.92
IRB	61.06	0.23	6.07	1.91	0.07	0.07	0.08	0.07	4.03
IRC	61.45	0.14	3.05	0.6	0.07	0.05	0.11	0.04	5.93
IIB	51.00	0.17	22.34	1.02	0.06	0.04	0.08	0.04	3.24
ILIB	52.48	0.22	14.51	3.75	0.06	0.15	0.09	0.09	5.4
IMB	44.33	1.52	25.1	2.04	0.07	0.1	0.09	0.1	5.27
IPB	36.17	0.13	44.08	0.78	0.05	0.03	0.07	0.05	2.45
IPC	38.12	0.1	41.05	0.56	0,000	0.02	0.04	0.03	3.14
ILPB	36.7	0.16	36.45	3.05	0.06	0.12	0.11	0.06	4.53
Average	52.76	0.28	18.12	1.50	0.06	0.06	0.08	0.06	3.60

The database analyzed over 370 meters of rock chemically classified as intermediate-manganese itabirite, within 34 different sampling intervals. Manganese itabirite is defined as those with a manganese percentage greater than or equal to 1%. A distinctive physical characteristic of this lithology is the presence of dark bands that appear more purplish compared to those typically rich in hematite. Manganese itabirites are considered iron ore, yet they exhibit significant variability in the range of iron percentage. Intermediate-manganese itabirite (IMB) typically exhibits medium values for silica, aluminum (Al), phosphorus (P), and calcium (Ca), with slightly higher levels of magnesium (Mg). Conversely, titanium shows the highest average concentration among all lithotypes.

Limonitic itabirites, historically referred to as dolomitic or clayey, are banded rocks characterized by alternating iron-rich bands and clayey-silty bands typically ocher in color, with a higher presence of clay minerals and consequently exceeding 2% aluminum content. Limonitic itabirites are further categorized based on their iron enrichment: intermediate limonitic itabirite (with iron content ranging from 45% to 58%) or poor limonitic itabirite (with iron content ranging from 20% to 45%), and by their compactness, which can be soft (density ranging from 2.3 to 2.6 g/cm³), semi-compact (density ranging from 2.4 to 2.8 g/cm³), or compact (density ranging from 2.9 to 3.0 g/cm³; refer to Table 4). These two lithotypes of limonitic itabirites exhibit distinct behaviors concerning their iron content. Intermediate limonitic itabirite (ILIB) contains an intermediate level of iron but a relatively low amount of SiO2, falling below the average for the sampled rocks. The concentrations of aluminum, calcium, titanium, and PPC are among the highest observed in this category (Table 4). On the other hand, poor limonitic itabirite (ILPB) exhibits the lowest iron content among all lithotypes. However, SiO_2, aluminum, calcium, titanium, and PPC levels register above-average values for the dataset (Table 4). These rocks exhibit iron content ranging from 45% to 58% in their composition. The percentages of manganese, silica, aluminum, phosphorus, calcium, magnesium, titanium, and PPC fall within the average range observed for the sampled lithotypes (Table 4).

Itabirites from the Moeda Syncline are presently categorized as rich when they possess an overall iron content ranging between 58% and 64%, accompanied by a density close to 2.9 g/cm³ for soft rocks and 3.6 g/cm³ for compact rocks. The order of enrichment of the other elements and oxides follows a similar pattern, with magnesium being more abundant than phosphorus, differing only in the inversion of CaO with TiO_2 as the most depleted element.

Samples with a chemical analysis indicating an overall iron percentage exceeding 64% are classified as hematite, with estimated densities of around 3.2 g/cm³ for friable samples, 3.5 g/cm³ for semi-compact samples, and 4.3 g/cm³ for compact hematite samples. These three lithotypes exhibit the highest iron content enrichment and consist predominantly of hematites. They typically demonstrate extremely low silica contents, with aluminum exhibiting average values (except for HEC, which shows low aluminum values).

Phosphorus, calcium, magnesium, and titanium levels fall within the expected average range (Table 4).

Mineral chemistry analysis

With the aim of evaluating chemical behavior, Harker-type graphs were generated using data from Fe, Al, and Mn, which are the elements with the highest concentration averages (excluding SiO_2), to illustrate their correlations with other elements (Figure 4). The dataset comprises a significant amount of information, often leading to trends being overshadowed by the sheer volume of data.

Figure 4 depicts the relationship between %Fe and other oxides. Al_2O_3, CaO, and TiO_2 exhibit subtle variations with an increase in %Fe. An inverse relationship exists between %Fe and SiO_2, as well as %Fe and MgO. Meanwhile, Mn and P show insignificant variation.

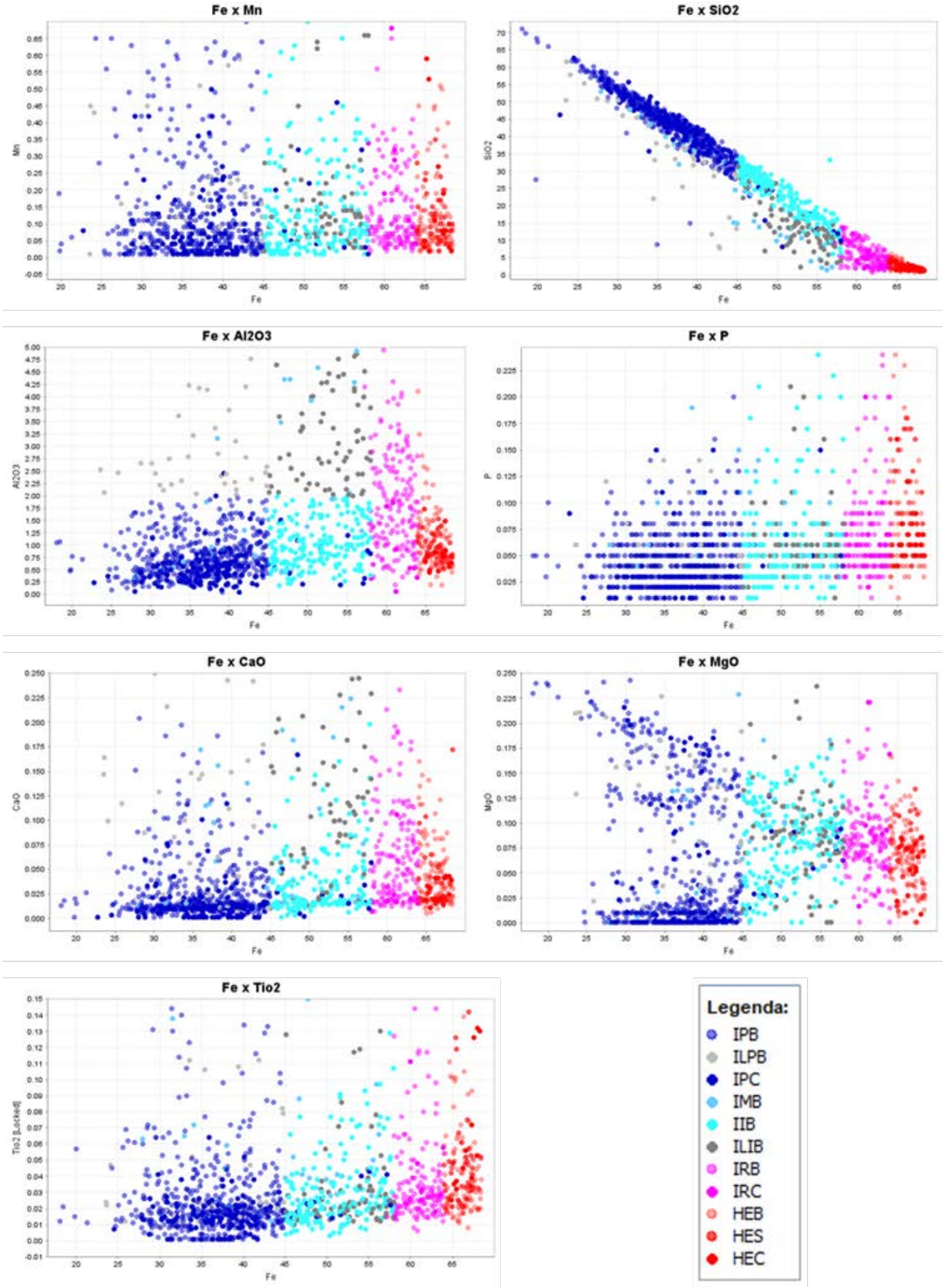

Figure 4 - Hacker diagrams showing the compositional difference between the iron ore lithotypes. Plots of major elements (wt.%).

In figure 5, different box plots illustrate the increasing enrichment order of various lithotypes for each oxide and major element. IMB notably demonstrates a mean Mn concentration above 1%, whereas the others display concentrations up to 10 times lower with minimal variation. Among

aluminum, the limonite itabirites ILPB and ILIB exhibit the highest richness. IRB, representing iron-rich itabirites, demonstrates the highest enrichment in Al.

The enrichment pattern in phosphorus indicates that means among different lithotypes are similar, yet there is enrichment in the richer ores (hematites and rich itabirites) compared to poorer itabirites.

Lithotypes with the highest CaO content are the limonitic and manganese-rich ones, whereas for TiO2, there is minimal variation in percentage, with slightly higher average quantities found in hematites and IMB. IPB and IPC are the least enriched lithotypes in all major elements (except for SiO_2, where they are the most enriched) when observing the enrichment sequence in the box plots for all elements

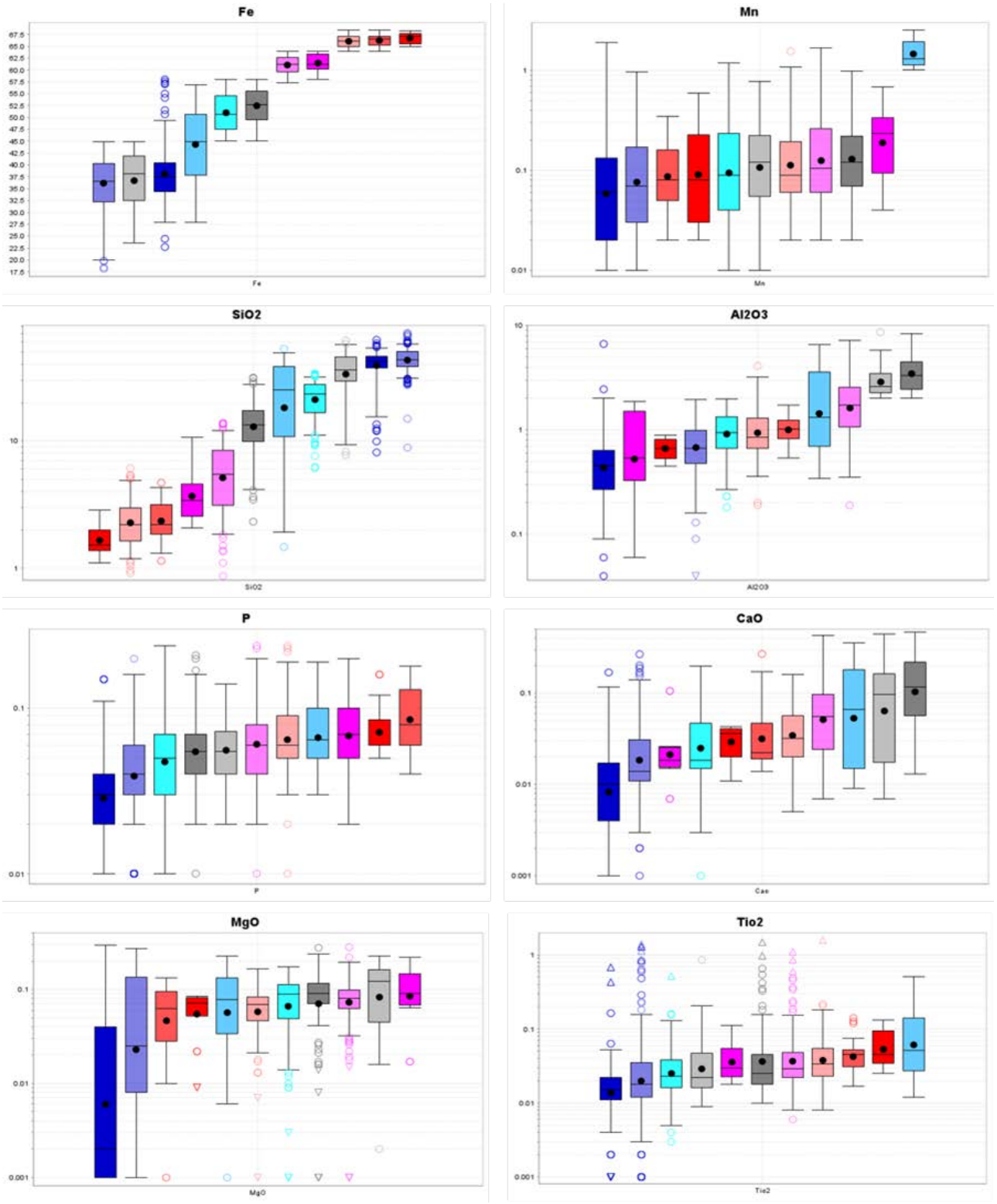

Figure 5 - Box plots showing the distribution of values for each element by lithotype

X-Ray Diffraction (XRD)

The phases identified on three BIF ore samples (Soft Poor Limonite Itabirite – ILPB, Soft Rich Manganese Itabirite – IMB, Soft Intermediate Limonite Itabirite – ILIB) and respective references of crystallographic information files are the following: quartz (Ikuta et al., 2007), hematite (Sawada, 1996), goethite with Al substitution (Li et al., 2006) and kaolinite (Bish & von Dreele, 1989), all available at the Crystallographic Open Database (COD). Diffraction peaks of these minerals show minimal overlap, which supports XRD analysis. The results of ILPB analysis of sample TG003-01 indicated the existence of goethite (59.9%) and quartz (39.5%) as largely predominant mineral phases in the limonitic band. In addition to them, there is the occurrence of a small fraction of kaolinite (0.6%). For sample TG004, XRD analysis revealed the presence of four mineral phases, the predominant ones being goethite (72.2%) and hematite (13.5%), mineral phases containing Fe.

Additionally, kaolinite (9.5%) and quartz (4.8%) were identified, as depicted in figures 6 and 7.

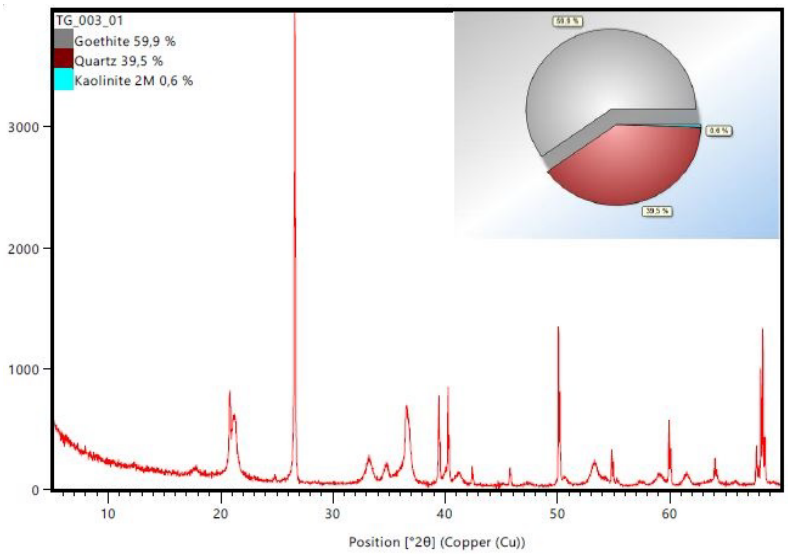

Figure 6 - X-ray diffractogram of TG003-01 sample.

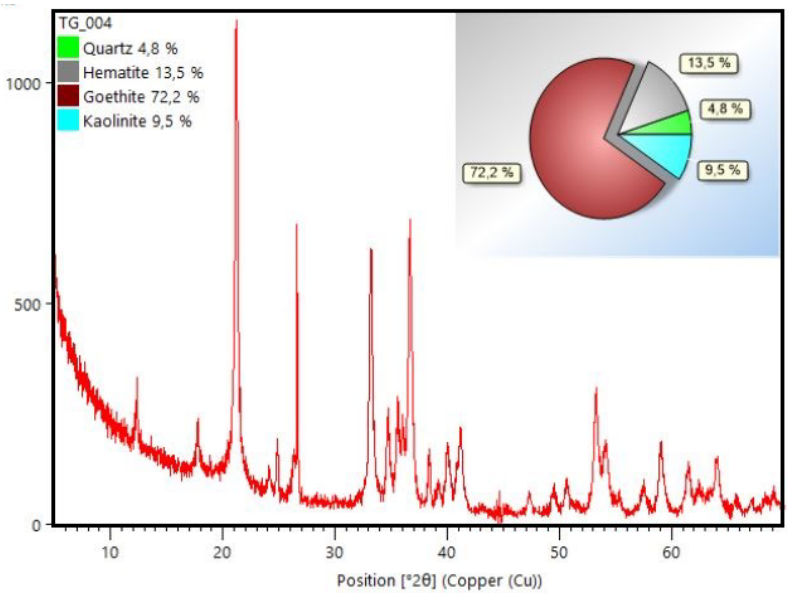

Figure 7 - X-ray diffractogram of TG004-01 sample

The XRD analysis of sample TG001 (Figure 8) revealed the predominance of mineral phases rich in Fe, primarily represented by goethite (67.9%) and hematite (24.5%). Additionally, kaolinite (6.7%) and quartz (0.9%) were detected to a lesser extent. For sample TG002, the analysis indicated the presence of three mineral phases, with a predominance of Fe-rich minerals, namely goethite (52.2%) and hematite (40.5%), along with quartz (7.3%) (Figure 9).

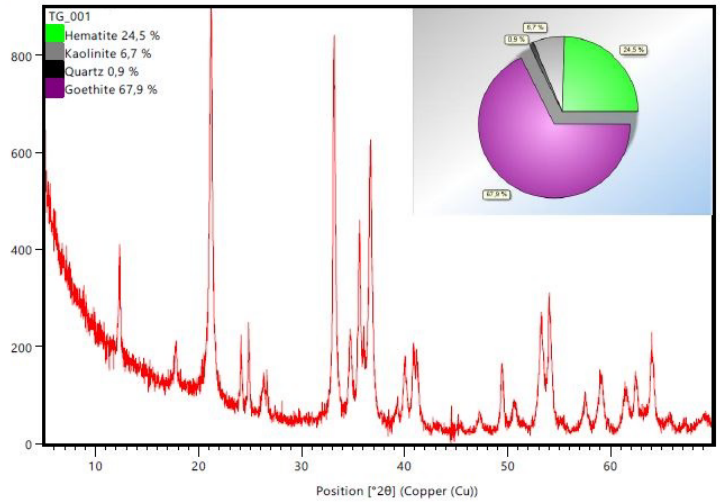

Figure 8 - X-ray diffractogram of TG001 sample

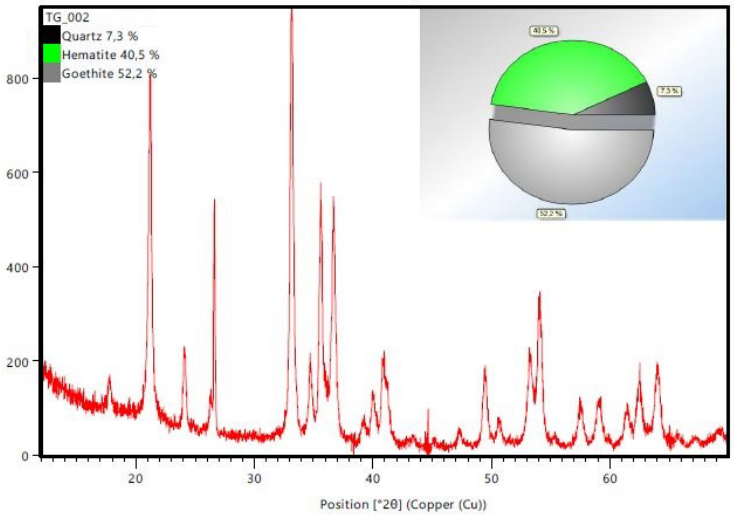

Figure 9 - X-ray diffractogram of TG002 sample

The TG006-06 corresponds to the mixture of bands enriched in Fe, limonitic bands, and siliceous bands, while the TG006-07 corresponds to the portion consisting only of enriched bands and limonitic bands. In the analysis of sample TG006-07, the result also indicated the occurrence of four mineral phases, similar to those observed in sample TG006-06: quartz (41.7%), hematite (23.4%), kaolinite (17.7%), goethite (17.2%), as shown in figures 10 and 11.

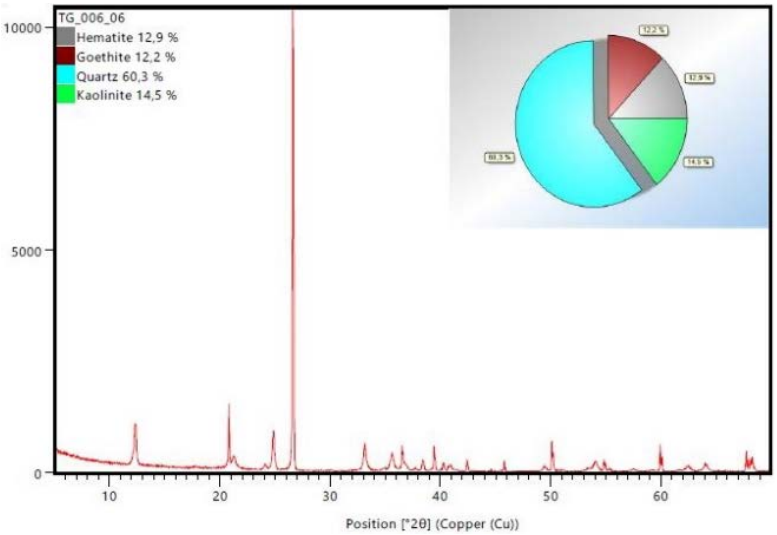

Figure 10 - X-ray diffractogram of TG006-6 sample

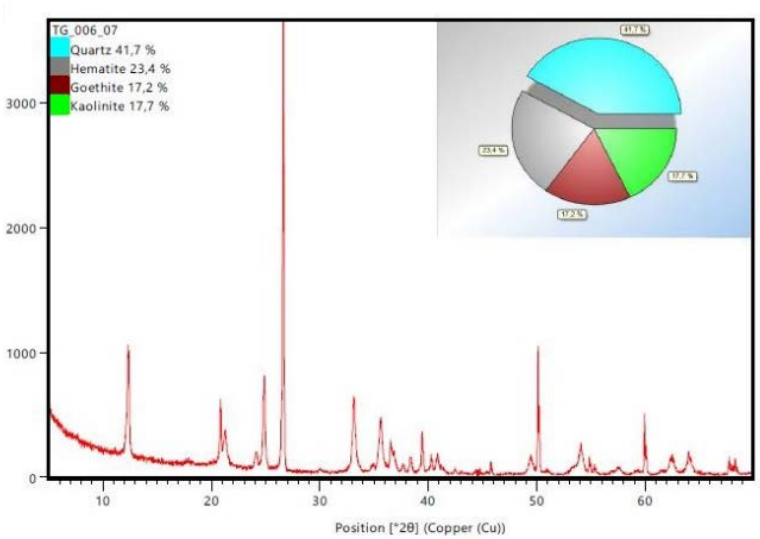

Figure 11 - X-ray diffractogram of TG006-7 sample

RESULTS AND DISCUSSIONS

Petrology

Iron oxide abundances generally increase upwards, with the upper horizons (ferruginous saprolite and lateritic residuum) largely composed of kaolinite, goethite, and hematite (Anand & Butt, 2010). But, in some cases, BIFs present anomalous enrichments in Iron hydroxides. Both situations will be discussed below.

Limonite Itabirites

The mineralogy of limonitic itabirites composition confirms the XRD, which pointed to the wide occurrence of quartz and goethite, with goethite being correlated in lamina to the limonite matrix. The presence of Fe oxides is not detected by XRD and is also rarely seen in the TG003-03 slide. The absence of oxides and the predominance of quartz are indicators of a low Fe content in the limonite band. Finally, the description of the bands enriched in Fe (sample TG004-02) confirms the abundance of oxides surrounded by a very fine earthy matrix of hydroxides, with only a small fraction of the material composed of quartz. The magnifying glass mineralogical descriptions of both bands show that the enriched bands are responsible for the high content of Fe oxides, while the limonitic bands represent the portion depleted in Fe and with a high content of SiO_2.

The sample TG006-05 exhibits mineralogy composed basically of quartz (around 70%) and hematite (20%), therefore indicating a broad dominance of quartz disseminated throughout the sample, accompanied by a low relative content of mineral phases rich in Fe, which differs from the field description. Another aspect highlighted by microscopy is the low expressivity of goethite and limonitic material, which make up less than 10% of the mineralogical fraction of the blade, different from what is commonly observed in limonitic itabirites in the mine, in which the abundance of goethite and limonite, mainly related to to the finest fractions of the rock. In addition to quartz, Fe oxides are described mainly in the Fe-rich band and the siliceous band, making up around 25% of both samples, which confirms the low Fe enrichment of the itabirite. In turn, hydroxides are concentrated especially in the limonite band, associated with quartz and rare oxide grains, in a composition similar to that described in the limonite band sample TG003-01. XRD indicates the presence of a considerable amount of kaolinite in both analyses carried out.

The description of the three petrographic slides prepared (TG009, TG010, and TG011) show mineralogy characterized by the predominance of hydrated Fe mineral phases (goethite and limonite). According to Hensler et al. (2017), these mineral phases are indicators of the action of supergene processes and can form horizons up to 80 m deep in the Moeda Syncline. A similar occurrence of hematite is recognized by Mendes (2015) at the Pau Branco Deposit and is interpreted as being of secondary origin, from the oxidation of magnetite crystals to hematite.

Manganese Itabirite

A broad dominance of limonite matrix (85%) is observed, which subordinately involves goethite crystals and, to a lesser extent, hematite and fine micas. The described composition shows the predominance of hydrated Fe mineral

phases. In turn, some samples are significantly enriched in Fe. This enrichment is evidenced by the increase in the proportion of hematite and goethite crystals, accompanied by a reduction in the limonite fraction.

When correlating the petrographic description with the XRD results, we can see both the increase in the hematite content and consequent enrichment in Fe, as well as the broad predominance of hydrated Fe mineral phases. The presence of micaceous minerals, together with the detection of clay minerals, may, however, indicate an abundance of Al_2O_3.

Itabirites

The described mineralogy proves the Fe impoverishment of the limonitic band about the enriched band, as discussed for limonitic itabirites. Unlike the itabirites discussed in these items, itabirites do not have quartz associated with limonitic bands, indicating a lower SiO2 content than in limonitic itabirites and, therefore, an ore with a higher Fe content (Grossi-Sad, 2005).

The mineralogical composition is indicative of the lithotype's high Fe and low SiO_2 content, confirming the Fe enrichment and good quality of the ore suggested in the field. Few samples are distinguished by the broad predominance of goethite (60%) over hematite (25%) and small enrichment in limonite.

Mendes (2015) argues that the contact between itabirite and intrusive rocks represents a zone of discontinuity that would facilitate the percolation of fluids, resulting in the hydration of Fe oxides.

Geochemistry

The average total chemistry values for each lithotype were normalized to the average values of the Upper Continental Crust (CCS), proposed by Taylor & McLennan (1995; Table 5; Figure 12) and shows a large variation of the elements concerning the crustal average, indicating a differentiation of the mine's lithotypes, possibly due to hydrothermal processes. As they are itabirites and Fe ore, the samples present a logical enrichment in Fe of around 10 times greater with the crust and are accompanied by an impoverishment in Si. This relationship is inverse between Fe and Si and is noted by the difference between the values, being very accentuated for the rich hematites and itabirites and softer for the other itabirites. In addition to Fe, the only elements with enrichment above the CCS average are Mn and P. The average Mn values of all lithotypes are slightly above the crustal standard, except for the manganese itabirite, which presents an average enrichment of 10 times greater than the crustal average. P values are concentrated just above the crustal value, except for the poor itabirites (IPC and IPB), with averages almost equal to or below the crustal average. Among the values below the CCS standard are Al, Ca, Mg, and Ti. The last three show little variation between lithotypes, being 10 to 100 times more depleted than the standard value. Al, on the other hand, is impoverished by around 10 times, except in the poor and intermediate limonitic itabirites, which show a slightly greater enrichment in the element.

Some samples analyzed in this work were plotted together with the percentage averages of each lithotype in the Fe_2O_3-$2Al_2O_3$-SiO_2 ternary diagram (Figure 13) used to classify itabirites from the Hamersley Province, Western Australia (Webb et al., 2003).

Table 5 - Average whole-rock chemical composition of database lithotypes and upper continental crust (CCS). CCS values are based on Taylor & McLennan (1995).

	HEB	**HEC**	**HES**	**IIB**	**ILIB**	**ILPB**	**IMB**	**IPB**	**IPC**	**IRB**	**IRC**	**CCS**
Fe	66,06	66,72	66,23	51,00	52,48	36,70	44,33	36,17	38,11	61,06	61,45	3,50
Mn	0,19	0,16	0,11	0,17	0,22	0,18	1,52	0,15	0,12	0,23	0,26	0,08
SiO_2	2,50	1,70	2,48	22,34	14,51	36,45	25,10	44,08	41,05	6,07	4,21	66,60
Al_2O_3	1,07	0,68	1,04	1,02	3,75	3,05	2,04	0,78	0,56	1,91	0,79	15,40
P	0,07	0,08	0,09	0,06	0,06	0,06	0,08	0,05	0,03	0,07	0,08	0,04
CaO	0,04	0,03	0,04	0,03	0,15	0,12	0,10	0,03	0,02	0,07	0,03	3,60
MgO	0,07	0,06	0,06	0,08	0,09	0,11	0,09	0,07	0,04	0,08	0,10	2,50
TiO_2	0,06	0,06	0,05	0,03	0,09	0,06	0,10	0,05	0,03	0,07	0,04	0,60

The first grouping converges with the field of BIFs defined by Webb et al. (2003) and corresponds mainly to the itabirites less enriched in Fe, while the second focuses on the Fe_2O_3 vertex and encompasses the rich itabirites and Fe ores. The furthest point from the Fe_2O_3, carried

out only in the limonitic pelitic band and correlated to the black shales field, which appears coherent considering the depletion in Fe and high silica content from this sample.

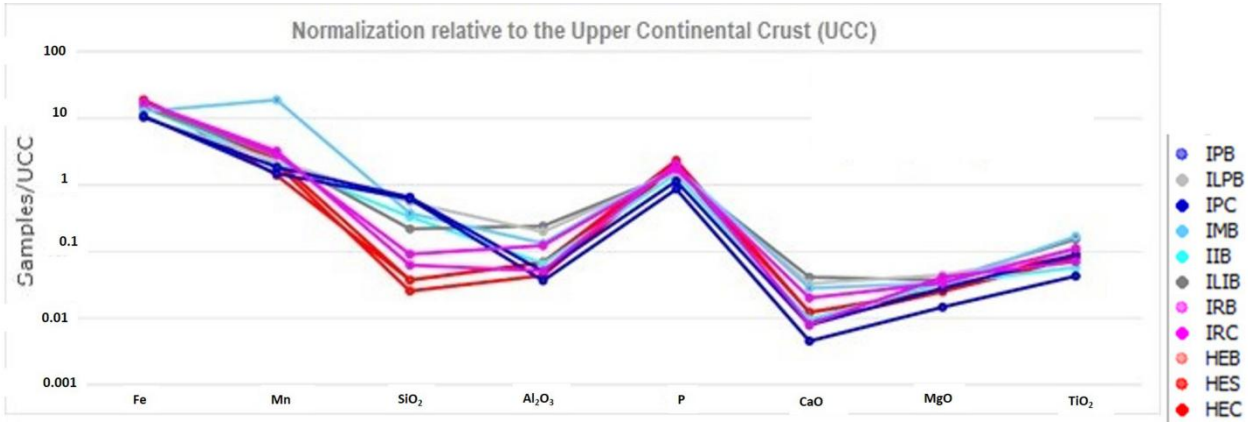

Figure 12 - Graph of the average values of each lithotype normalized by CCS (Taylor & McLennan, 1995).

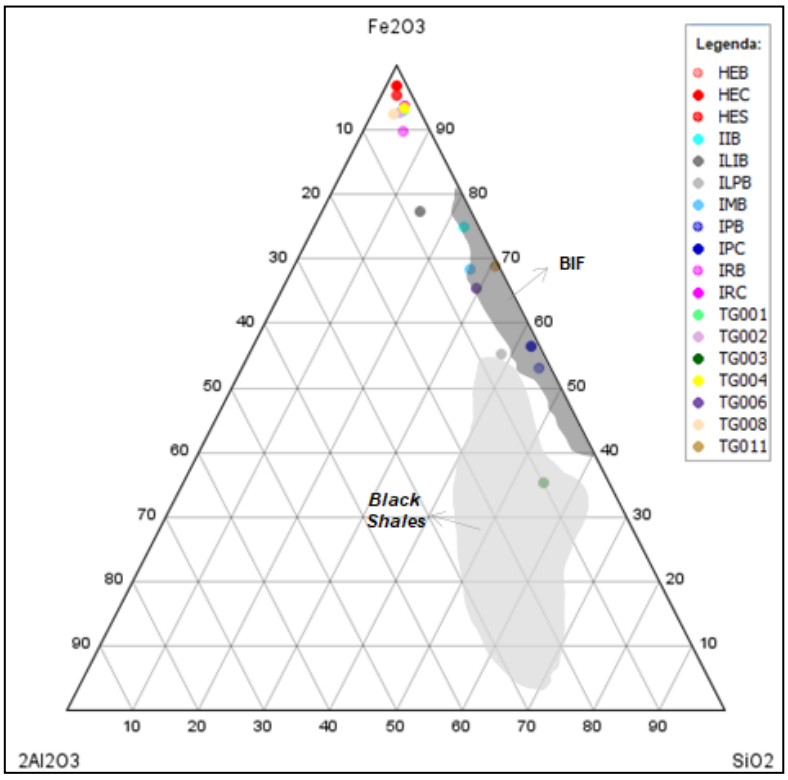

Figure 13. Ternary diagram for geochemical classification of banded iron formations (BIFs) and black shales.

Given the results of the chemical analyses, it became possible and necessary to reclassify/ reframe the lithologies, previously recognized by the lithology identified in the field according only to their main physical characteristics. However, according to the percentages of Fe, Mn, and Al_2O_3 and following table 2, which defines the ore lithotypes according to these elements, the samples were reclassified according to table 6.

Regarding hydrothermal processes, interpretations by several authors mention that mineralization at the Moeda Syncline is influenced by a set of both hypogenic and supergenic processes, responsible for the Fe enrichment in the deposit (Rosière et al., 2008; Mendes, 2015; Hensler et al., 2017).

To investigate the action of hydrothermal processes in BIFs in the studied deposit, two graphs were used by Sylvestre et al. (2017) to characterize the Kouambo Fe deposit (Figures. 14 and 15).

The first graph analyzed is Al vs. Si (Figure 14). As evidenced in the graph, most samples and percentage averages fall below the hydrothermal field, except for the poor itabirites (IPC and IPB). This relationship is coherent since low Fe contents are accompanied by higher Si contents.

Table 6 - Reclassification of the lithotype of the collected samples, according to chemical analysis and percentages of Fe, Mn and Al_2O_3.

Sample	Iron Ore Lithotype	%Fe	%Mn	%Al_2O_3	Reclassified Lithotype
TG001	Soft Rich Manganese Itabirite (IMB)	60,64	0,30	1,04	Soft Rich Itabirite (IRB)
TG001	Soft Rich Manganese Itabirite (IMB)	61,18	0,25	1,32	Soft Rich Itabirite (IRB)
TG002	Soft Rich Manganese Itabirite (IMB)	61,31	0,30	1,28	Soft Rich Itabirite (IRB)
TG002	Soft Rich Manganese Itabirite (IMB)	60,65	0,29	1,68	Soft Rich Itabirite (IRB)
TG003	Soft Poor Limonite Itabirite (ILPB)	24,13	0,19	4,83	Soft Poor Limonite Itabirite (ILPB)
TG004	Soft Poor Limonite Itabirite (ILPB)	58,87	0,12	0,91	Soft Rich Itabirite (IRB)
TG006	Soft Intermediate Limonite Itabirite (ILIB)	46,07	0,14	2,55	Soft Intermediate Limonite Itabirite (ILIB)
TG008	Semi-compact Intermediate Itabirite (IIS)	64,00	0,13	2,03	Semi-compact Hematite (HES)
TG011	Compact Intermediate Limonite Itabirite (ILIC)	46,25	0,23	0,15	Semi-compact Intermediate Itabirite (IIS)

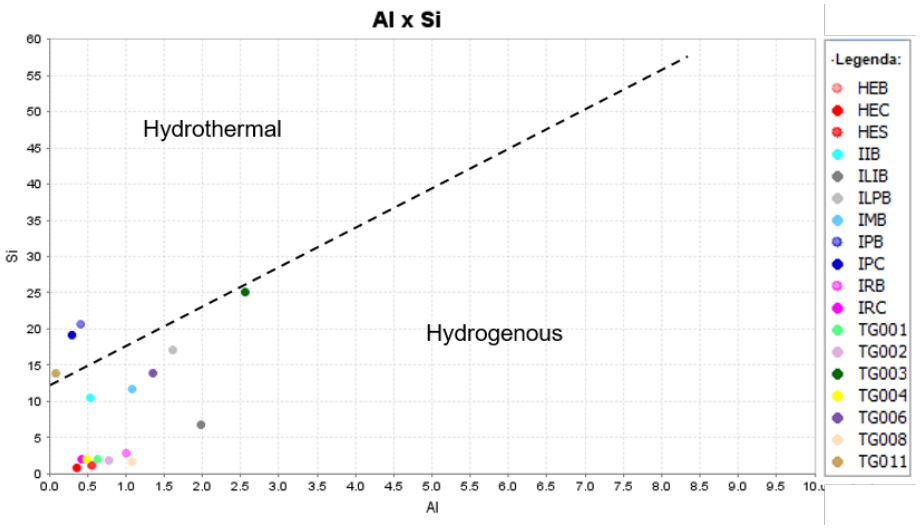

Figure 14 - Al x Si graph indicating little hydrothermal affinity of the BIFs studied (Modified from Sylvestre et al., 2017).

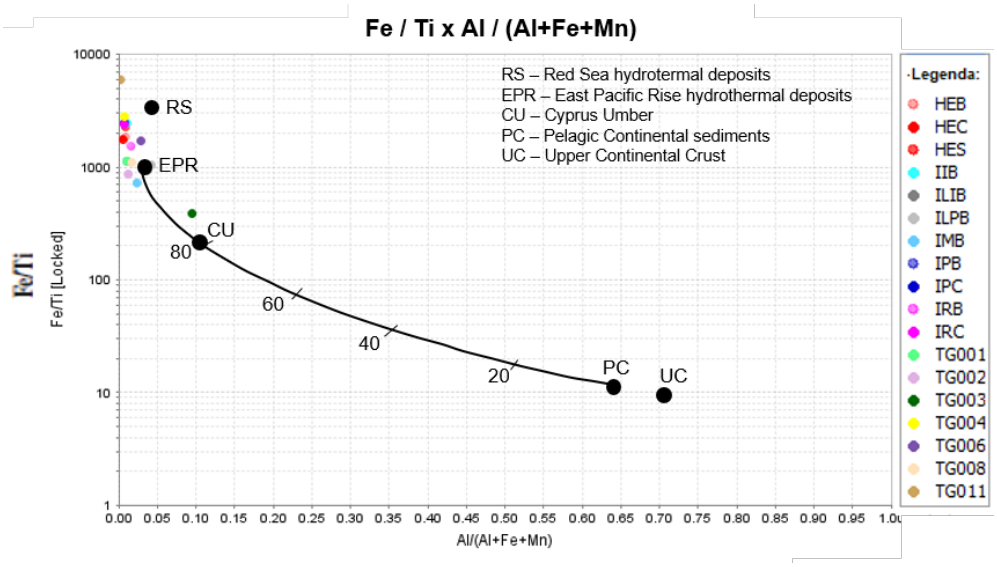

Figure 15 - Fe/Ti x Al/(Al+Fe+Mn) diagram, indicating geochemical affinity of the studied BIFs with hydrothermal deposits in the Red Sea and the Pacific Ocean (Modified from Sylvestre et al., 2017).

From the graph, a low hydrothermal contribution is suggested, corroborated by Mendes (2015), who states that hydrothermalism did not significantly affect the composition geochemistry of itabirites.

The second graph discussed is presented in figure 15 and is based on the premise that contamination of the deposit by pelagic sediments

enriches the system in Ti and Al (Sylvestre et al., 2017).

This interpretation diverges from the interpretation of the previous graph (Figure 14), suggesting the impossibility of defining the hydrothermal contribution only through the largest elements.

XRD Analysis

X-ray diffraction (XRD) analysis revealed that the limonitic band is composed mainly of goethite (59.9%) and quartz (39.5%), with a small amount of kaolinite. This indicates the dominant presence of hydrated iron phases, represented by goethite, accompanied by a high proportion of siliceous mineral phases, mainly quartz. The XRD analysis did not reveal the presence of typical manganese-bearing minerals above the detection limit.

This indicates a positive correlation between kaolinite and goethite in XRD analyses. The absence of bands rich in SiO_2 reduces the proportion of quartz in the sample.

Therefore, there is an inverse correlation between iron enrichment and the presence of siliceous bands. In other words, the higher the abundance of quartz, the lower the expected content of hematite and goethite in the XRD analysis. Discrepancies, in conclusion, are possibly related to the presence of poorly crystallized phases, particularly goethite, which causes a slight underestimation of Fe contents by XRD analysis.

CONCLUSION

The obtained data, studies, and discussions allow us to conclude that there is a high degree of weathering alteration in the rocks, evidenced by the abundance of hydrated Fe phases and the low preservation of primary structures, as observed in the microscope.

The deposit mineralogical characterization confirms the proposed deposit paragenesis by Hensler et al. (2017), as hematites martitized originating from the alteration of magnetites were observed, which later transformed into goethite.

Therefore, a reclassification was generated for all necessary samples based on the observed rock characteristics in the field aligned with their chemical composition, showing that despite the presence of impurities such as Al and Mn, more commonly found in limonite and manganese itabirites respectively, these lithotypes will commonly be considered ore due to their high Fe content, as seen in the database analysis and the collected samples.

ACKNOWLEDGEMENTS

Acknowledgement is made to the numerous employees of Vallourec Mineração that have supported the research. Dra. Flávia Silveira Braga (UFMG) e Dr. Igor Santana (CPMTC-UFMG) are thanked for comments, whose contributions are gratefully acknowledged. The authors would also like to Centro de Pesquisa Manoel Teixeira da Costa (CPMTC-UFMG) for support in sample analysis.

REFERENCES

ALKMIM, F.F. & MARTINS-NETO M.A. Proterozoic first-order sedimentary sequences of the São Francisco craton, eastern Brazil. **Marine and Petroleum Geology**, v. 33, n. 1, p. 127-139, 2012.

ALMEIDA, F.F.M.; HASUI, Y.; BRITO NEVES, B.B. The Upper Precambrian of South America. Boletim. **Instituto de Geociências USP**. São Paulo, v. 7, p. 45-80, 1976

ANAND, R.R. & BUTT, C.R.M. A guide for mineral exploration through the regolith in the Yilgarn Craton, Western Australia. **Aust. J. Earth Sci**. v. 57, p. 1015–1114, 2010.

BABINSKI, M.; CHEMALE JR., F.; SCHUMUS, W. R. Geocronologia Pb/Pb em rochas carbonáticas do Supergrupo Minas, Quadrilátero Ferrífero, Minas Gerais, Brasil. In: CONGRESSO BRASILEIRO DE GEOQUÍMICA, 3., São Paulo, 1991. **Anais**... São Paulo: Sociedade Brasileira de Geoquímica, v. 2, 1991, p. 628-630.

BABINSKI, M.; CHEMALE JR., F.; SCHMUS, W.R.V. The Pb/Pb age of the Minas Supergroup carbonate rocks, Quadrilátero Ferrífero, Brazil. **Precambrian Research**, v.72, p. 235-245, 1995.

BALTHAZAR, O.F. & ZUCCHETTI, M. Lithofacies associations and strucutural evolution of the Archean Rio das Velhas greenstone belt, Quadrilátero Ferrífero, Brazil: A review of the setting of gold deposits. **Ore Geology Reviews,** v. 32, p. 471-499, 2007.

BISH, D.L. & VON DREELE, R.B. Rietveld refinement of non-hydrogen atomic positions in kaolinite. **Clays and Clay Minerals**, v. 37, n. 4, p. 289-296, 1989.

CABRAL, A.R.; ZEH, A.; KOGLIN, N.; GOMES JR., A.A.S.; VIANA, D.J.; LEHMANN, B. Dating the Itabira iron formation, Quadrilátero Ferrífero of Minas Gerais, Brazil, at 2.65 Ga: Depositional U-Pb age of zircon from a metavolcanic layer. **Precambrian Research**, v. 204, p. 40-45. 2012

CASTRO, P.T.A.; ENDO, I.; GANDINI, A.L. **Quadrilátero Ferrífero: Avanços do conhecimento nos últimos 50 anos**. 1ª Ed. 3i Ed. 480 p. 2020.

COSTA, M.F.; KYLE, J.R.; LOBATO, L.M.; KETCHAM, R.A.; FIGUEIREDO E SILVA, R.C.; FERNANDES, R.C. Orogenic gold ores in three-dimensions: A case study of distinct mineralization styles at the world-class Cuiabá deposit, Brazil, using high-resolution X-ray computed tomography on gold particles. **Ore Geology Reviews**, v. 140, p. 1-18, 2022.

DORR, J.N. II., GAIR J.E., POMERENE J.B., RYNEARSON G.A. **Revisão Estratigráfica Pré-Cambriana do Quadrilátero Ferrífero**. Rio de Janeiro, DNPM/DFPM. Avulso. 81, 36 p., 1957.

DORR, J.V.N. II. Physiographic, stratigraphic and structural development of the Quadrilátero Ferrífero, Minas Gerais, Brazil. U. S. **Geological Survey. Prof. Paper**, v. 641-A, 110 p. 1969.

GROSSI-SAD, J.H. Relatório final de avaliação da reserva da Mina Pau Branco. **V&M Mineração Ltda.** Estudo Técnico. 102 p., 2005.

HARTMANN, L.A.; ENDO, I.; SUITA, M.T.F.; SANTOS, J.O.S.; FRANTZ, J.C.; CARNEIRO, M.A.; MCNAUGHTON, N.J.; BARLEY, M.E. Provenance and age delimitation of Quadrilátero Ferrífero sandstones based on zircon U-Pb isotopes. **Journal of South American Earth Sciences**, v. 20, n. 4, p. 273-285, 2006.

HENSLER, A.S.; HAGEMANN, S.G.; BROWN, P.E.; ROSIÈRE, C.A. Using oxygen isotope chemistry to track hydrothermal processes and fluid sources in itabirite-hosted iron ore deposits in the Quadrilátero Ferrífero, Minas Gerais, Brazil. **Mineralium Deposita**, v. 49, p. 293-311, 2014.

HENSLER, A.S.; ROSIÈRE, C.A.; HAGEMANN, S.G. Iron Oxide Mineralization at the Contact Zone Between Phyllite and Itabirite of the Pau Branco Deposit, Quadrilátero Ferrífero, Brazil – Implications for Fluid-Rock Interaction During Iron Ore Formation**. Economic Geology**, v. 112, p. 941-982, 2017.

HERZ, N. **Gneissic and igneous rocks of the Quadrilátero Ferrífero, Minas Gerais, Brazil**. USGS/DNPM. Professional Paper 641-B. 57 p. 1970.

IKUTA, D.; KAWAME, N.; BANNO, S., HIRAJIMA, T.; ITO, K.; RAKOVAN, J.F.; DOWNS, R.T.; TAMADA, O. First in situ X-ray identification of coesite and retrograde quartz on a glass thin section of an ultrahigh-pressure metamorphic rock and their crystal structure details. **American Mineralogist**, v. 92, n. 1, p. 57-63, 2007.

KLEIN, C. & LADEIRA, E.A. Geochemistry and petrology of some Proterozoic banded iron-formations of the Quadrilátero Ferrífero, Minas Gerais, Brazil. **Economic Geology**, v. 95, p. 405- 428, 2000

KOGLIN, N., ZEH, A., CABRA, LA.R., GOMES, A.A.S., CORRÊA NETO, A.V., BRUNETTO, W.J., GALBIATTI, H. Depositional age and sediment source of the auriferous Moeda Formation, Quadrilátero Ferrífero of Minas Gerais, Brazil: New constraints from U-Pb-Hf isotopes in zircon and xenotime. **Precambrian Research, v.** 255(Part 1), p. 96-108, 2014.

LANA, C., ALKMIM, F.F., ARMSTRONG, R., SCHOLZ, R., ROMANO, R., NALINI JR. H.A. The ancestry and magmatic evolution of Archean TTG rocks of the Quadrilátero Ferrífero province, southeast Brazil. **Precambrian Research**, v. 231, p. 157-173, 2013.

MENDES, M.C.O. Gênese dos itabiritos e minérios hipogênicos do Quadrilátero Ferrífero com base em geoquímica e isótopos de ferro e geocronologia de rochas associadas. Belo Horizonte, 2015. 126 p. Tese (Doutorado), Universidade Federal de Minas Gerais.

MENDES, M., LOBATO, L.M., KUNZMANN, MIron isotope and REE+Y composition of the Cauê banded iron formation and related iron ores of the Quadrilátero Ferrífero, Brazil. **Miner Deposita,** v. 52, p. 159–180, 2017

LI, D.; O'CONNOR, H.; LOW I.; VAN RIESSEN, A.; TOBY, B.H. Mineralogy of Al-substituted goethites. **Powder Diffraction**, v. 21, 4, p. 289-299, 2006

RENGER, F.E.; NOCE, C.M.; ROMANO, A.W.; MACHADO, N. Evolução sedimentar do Supergrupo Minas: 500 Ma de registro geológico no Quadrilátero Ferrífero, Minas Gerais, Brasil. **Geonomos**, v. 2, n. 1, p. 1-11, 1994.

RONCATO, J., MARTINS, M.M.; SILVA, M.M.L. (). Remote sensing applied to geological, structural, and mass movements characterization in the connection between Curral Homocline and Moeda Syncline, Quadrilátero Ferrífero Region, Brazil. **Brazilian Journal of Geology**, v. 53, n. 1, p. e20220040, 2023.

RONCATO, J.; CARVALHO ALMEIDA, A.L.; MACEDO, B.; OLIVEIRA, M. A geophysical analysis of the conceição river region Quadrilátero Ferrífero, based on field, petrographic, aerial images and airborne data. **Geociências**, v. 39, n. 1, p. 47-63, 2020.

RONCATO. J.G.; LOBATO, L.M.; SILVA, R.C.F.E.; LIMA, L.C.; PORTO, C.G. Metaturbidite-hosted gold deposits, Córrego do Sítio lineament, Quadrilátero Ferrífero, Brazil. **Brazilian Journal of Geology**, v. 45, p. 5-22, 2015.

ROSIÈRE, C.A.; SPIER, C.A.; RIOS, F.J.; SUCKAU, V. E. The itabirites of the Quadrilátero Ferrífero and related high-grade iron ore deposits: an overview. **Society of Economic Geologists Reviews**, v. 15, p. 223-254, 2008.

SAWADA, H. An electron density residual study of α-ferric oxide. **Materials Research Bulletin**, v. 31, n. 2, p. 141-146, 1996.

SEPULVEDA, G.O.; NOVO, T.A.; RONCATO, J. Characterization and geochronology of Archean metasedimentary sequences in the eastern portion of Rio das Velhas greenstone belt, Quadrilátero Ferrífero, Brazil. **Journal of South American Earth Sciences**, v. **105**, p. 102962, 2021.

SCHORSCHER, H.D. Polimetamorfismo do Pré-Cambriano na região de Itabira, Minas Gerais. XXXIX CONGRESSO BRASILEIRO DE GEOLOGIA, Ouro Preto, MG. **Resumos**...Ouro Preto: Sociedade Brasileira de Geologia, 1976. p. 194-195.

SCHORSCHER, H.D.; CARBONARI, F.C.; POLONIA, J.C.; MOREIRA, J.M.P., Quadrilatero Ferrtfero-Minas Gerais State: Rio das Velhas greenstone belt and Proterozoic rocks. In: INTERN. SYMP. EARLY ARCH. PROT., Salvador, 1982. Annex Excur…Salvador: Sociedade Brasileira de geologia, 46 p., 1982.

SOUSA, D.V.M. **Estudo geoquímico-mineral das formações ferríferas bandadas do Sinclinal Gandarela, Quadrilátero Ferrífero (MG).** Ouro Preto, 2016, 85 p. Dissertação (Mestrado). Universidade Federal de Ouro Preto.

SOUZA, P.C. & MÜLLER, G. Primeiras estruturas algais comprovadas na Formação Gandarela, Quadrilátero Ferrífero. **Revista da Escola de Minas**, v. 37, p. 13–21, 1984.

SYLVESTRE, G.; LAURE, N.T.E.; DJUBRIL, K.N.G.; ARLETTE, D.S.; CYRIEL, M.; TIMOLÉON, N.; PAUL, N.J. A mixed seawater and hydrothermal origino f superior-type banded iron formation (BIF)-hosted Kouambo iron deposit, Paleoproterozoic Nyong series, Southwestern Cameroon: Constraints from petrography and geochemistry. **Ore Geology Reviews**, v. 80, p. 860-875, 2017.

TAYLOR, S.R. & MCLENNAN, S. M. The geochemical evolution of the continental crust. **Reviews of Geophysics,** v. 33, p. 241-265, 1995

ZUCCHETTI, M. & BALTAZAR, O.F. Rio das Velhas Greenstone Belt lithofacies associations, Quadrilátero Ferrífero, Minas Gerais, Brazil. In: 31th INTERNATIONAL GEOLOGICAL CONGRESS, Rio de Janeiro, Brazil, **Actas**...Rio de Janeiro: Sociedade Brasileira de **Geologia,** CD-ROM. 2000

WEBB, A.D.; DICKENS, G.R.; OLIVER, N.H.S. From banded iron formation to iron ore: geochemical and mineralogical constraints from across the Hamersley Province, Western Australia. **Chemical Geology**, v. 197, p. 215-251, 2003.

Submetido em 8 de maio de 2024
Aceito para publicação em 25 de agosto de 2024